

Specific heat and thermal conductivity in the vortex state of the two-gap superconductor MgB₂

L. Tewordt and D. Fay

I. Institut für Theoretische Physik, Universität Hamburg, Jungiusstr. 9, 20355 Hamburg, Germany

(May 21, 2019)

The specific heat coefficient $\gamma_s(H)$ and the electronic thermal conductivity $\kappa_{es}(H)$ are calculated for Abrikosov's vortex lattice by taking into account the effects of supercurrent flow and Andreev scattering. First we solve the gap equation for the entire range of magnetic fields. We take into account vertex corrections due to impurity scattering calculated in the Born approximation. The function $\gamma_s(H)/\gamma_n$ increases from zero and becomes approximately linear above $H/H_{c2} \sim 0.1$. The dependence on impurity scattering is substantially reduced by the vertex corrections. The upward curvature of $\kappa_{es}(H)/\kappa_{en}$, which is caused by decreasing Andreev scattering for increasing field, is reduced for increasing impurity scattering. We also calculate the temperature dependence of the scattering rates $1/\tau_{ps}(H)$ of a phonon and $1/\tau_{es}(H)$ of a quasiparticle due to quasiparticle and phonon scattering, respectively. At low temperatures the ratio $\tau_{pn}/\tau_{ps}(H)$ increases rapidly to one as H tends to H_{c2} which yields a rapid drop in the phononic thermal conductivity κ_{ph} . Our results are in qualitative agreement with the experiments on the two-gap superconductor MgB₂.

I. INTRODUCTION

Although superconductivity in MgB₂¹ has been established as conventional phonon-mediated s-wave superconductivity, it is often difficult to analyze the results of measurements of various physical quantities because there exist two gaps of different magnitude associated with different bands. Their ratio is estimated as $r = \Delta_0^S/\Delta_0^L \sim 0.3 - 0.4$ where the larger gap Δ_0^L is associated with the two-dimensional σ -bands and the smaller gap Δ_0^S with the three-dimensional π -bands. Evidence for two gaps is provided by the rapid rise of the specific heat coefficient $\gamma_s(H)$ at very low fields.^{2,3} Recent measurements of the in-plane thermal conductivity $\kappa_s(H)$ for fields both parallel and perpendicular to the c-axis provide more evidence for the existence of two gaps because they show a very unusual field dependence at low temperatures.⁴ For increasing field, $\kappa_s(H)$ drops rapidly and reaches a minimum at a relatively low field, then exhibits an S-shape behavior where a steep rise in the low-field region is followed by a downward curvature up to about $H_{c2}/2$ and finally an upward curvature near H_{c2} for $\mathbf{H} \parallel \mathbf{c}$. The initial drop is attributed to the decrease of the phononic contribution $\kappa_{ph}(H)$ which is caused by the rapid enhancement of scattering of phonons by the quasiparticles in the vortex cores associated with the π -band. The steep increase in the low field region is attributed to the rapid rise of the electronic contribution $\kappa_e(H)$ which arises from the rapid release of mobile quasiparticles in the vortex lattice associated with the π -band. The final upward curvature of $\kappa(H)$ near H_{c2} for $\mathbf{H} \parallel \mathbf{c}$ is presumed to be due to the mobile carriers of the vortex lattice associated with the σ -band.

The field dependence of $\gamma_s(H)$ and $\kappa_{es}(H)$ can be explained qualitatively in terms of a two-band model with two energy gaps of different magnitude in the two bands where the band with strong pairing (the L, or σ -band) is responsible for the superconductivity and the superconductivity in the second band (the S, or π -band) is induced by Cooper pair tunneling.⁵ The vortices in the S-band have large vortex cores of radius ξ_0^S and already start to overlap in weak fields. This leads to a strong suppression of the small gap at a "virtual" upper critical field $H_{c2}^S \sim 3 - 4$ kOe which is much smaller than $H_{c2}^{(c)} \simeq 35$ kOe. The large radius of the vortex core and the field-induced suppression of the smaller gap is consistent with recent scanning tunneling spectroscopy (STS) measurements.⁶

Theories of the electronic thermal conductivity κ_e ⁷ and the phononic thermal conductivity κ_{ph} ⁸ in the mixed state have been developed on the basis of the Brandt-Pesch-Tewordt (BPT)⁹⁻¹¹ and the equivalent Pesch (P)¹² approximation schemes. Linear response equations for the vortex state¹³ yield another expression for κ_e which has been applied to d-wave pairing superconductivity in the cuprates.¹⁴ In the BPT-approximation the normal and anomalous Green's functions G and F are derived from Gorkov's integral equations with kernel $\Delta(r_1)G_{-\omega}^0(r_1 - r_2)\Delta^*(r_2)\exp(-i\int_1^2 2eA \cdot ds)$ where $\Delta(r)$ is Abrikosov's vortex lattice order parameter and $G_{-\omega}^0$ is the quasihole propagator. Thus these Green's functions take into account the effects of supercurrent flow and Andreev scattering

in the vortex cores as well as quasiparticle transfer between the vortices. The expression for κ_e ⁷, which has been derived from the Kubo formula in analogy to the procedure in Ref. 15, consists essentially of the ω -integral with the factor $(\omega/T)^2 \text{sech}^2(\omega/2T)$ determining the temperature dependence, the "destructive" coherence factor arising from the combination $(GG^\dagger - FF^\dagger)$, and the total scattering rate in the denominator consisting of the sum of the quasiparticle scattering rates γ and $\gamma_A(\omega, H)$ due to impurity and Andreev scattering. In the present paper we shall also calculate the scattering rate $1/\tau_{es}$ due to thermal scattering in the vortex state, but this becomes comparable to γ only at higher temperatures. The expression for κ_{ph} contains, in addition to the sum of scattering rates of phonons by different defects, the scattering rate $1/\tau_{ps}$ for phonons scattered by quasiparticles in the vortex state. The latter expression was obtained by replacing in the BCS-expression¹⁶ the density of states (DOS) and "coherence" functions by the expressions resulting from the P-approximation for the vortex state.⁸

The results for $\gamma_s(H)/\gamma_n$, $\kappa_{es}(H)/\kappa_{en}$, and τ_{pn}/τ_{ps} , which were obtained in Ref. 8 for a single cylindrical or spherical band and an isotropic s-wave pairing gap, turned out to depend sensitively on the reduced impurity scattering rate $\delta = \Gamma/\Delta_0 = (\pi/2)\xi_0/\ell$ where ξ_0 is the zero-field coherence length and ℓ is the mean free path. If one takes for the π -band in MgB₂ $\xi_\pi \sim 500\text{\AA}$ from the STS measurements⁶ and a mean free path $\ell_\pi \sim 500 - 800\text{\AA}$, one arrives at a reduced scattering rate $\delta_\pi \sim 1$ which is much larger than the largest value of $\delta = 0.5$ taken in Ref. 8. For such a large impurity scattering rate it is necessary to renormalize the impurity scattering self energy and to take into account the corresponding vertex corrections. The vertex corrections yield a renormalization of the gap function^{10,12} which, near H_{c2} , tends to the renormalization function which has been derived in the calculation of H_{c2} .¹⁷ It turns out that this gap renormalization substantially reduces the dependence of the functions $\gamma_s(H)/\gamma_n$, $\kappa_{es}(H)/\kappa_{en}$, and $\tau_{pn}/\tau_{ps}(H)$ on impurity scattering.

Recently it has been shown that numerical solutions of the Eilenberger equations yield a spatial average of the density of states (DOS) which is approximated very well by the DOS obtained with the BPT- and P-approximations over the whole field range between H_{c2} and H_{c1} .¹⁸ This result motivates us to calculate the field dependence of the central parameter of the theory, $\tilde{\Delta} = \Delta\Lambda/v$, from the gap equation in the P-approximation¹⁸ by including the impurity scattering vertex corrections in analogy to those in the gap equation of the BPT-approximation.¹⁰ Here Δ^2 is the spatial average of $|\Delta(r)|^2$ where $\Delta(r)$ is Abrikosov's vortex lattice order parameter, $\Lambda = (2eH)^{-1/2} = (\pi/2)^{1/2}a$ where a is the lattice constant of the vortex lattice, and v is the Fermi velocity perpendicular to the uniform field \mathbf{H} . It turns out that one can fit the exact results of these calculations very well with the relation between $\tilde{\Delta}^2$ and H/H_{c2} given by the Ginzburg-Landau relationship if one uses an appropriate value of the Abrikosov parameter $\beta_A = <|\Delta|^4> / (<|\Delta|^2>)^2$.

We have also investigated the temperature dependence of the phonon relaxation time ratio $\tau_{pn}/\tau_{ps}(H)$ and find that this ratio increases rapidly to one with increasing H in proportion to $[\gamma_s(H)/\gamma_n]^2$ for temperatures $T < (1/2)\Delta(T, H)$. This yields a rapid decrease of κ_{ph} for small fields and relatively low temperatures if one takes for Δ the small gap $\Delta^S(T, H)$ of the π -band. In this way one can explain the observed drop of κ for small fields and temperatures near $T_c/6$ which is attributed to the drop of κ_{ph} .⁴

Since the interband impurity scattering between the σ - and π -band is small,²⁰ one can add, in a crude approximation, our results obtained for a single isotropic gap in a cylindrical or spherical Fermi surface (FS) band by weighting them with the corresponding density of states. If one takes into account that the "virtual" upper critical field for the three-dimensional π -band is much smaller than the upper critical field of the two-dimensional σ -band,³ one can explain qualitatively the measured field dependence of the specific heat and thermal conductivity in MgB₂.

II. THEORY OF THE SPECIFIC HEAT AND ELECTRONIC AND PHONONIC THERMAL CONDUCTIVITY IN ABRIKOSOV'S VORTEX LATTICE

The basis of our theory is the approximation of Brandt, Pesch, and Tewordt (BPT)⁹⁻¹¹ for the normal and anomalous Green's functions G and F in the mixed state. A simplified version of this theory has been derived by Pesch (P)¹² from the quasiclassical Eilenberger equations. In this version the ε -integrals of the spatial averages of the spectral functions, $-\text{Im}G/\pi$ and $-\text{Im}F/\pi$, denoted by A and B , take on the following form:⁸

$$A(\Omega; \tilde{\Delta}, \theta) \equiv N(\omega, \theta)/N_0 = \text{Re} \left[1 + \frac{8\tilde{\Delta}_r^2}{\sin^2 \theta} [1 + i\sqrt{\pi} z w(z)] \right]^{-1/2}, \quad (1)$$

$$B(\Omega; \tilde{\Delta}, \theta) = \text{Re} \left[\frac{-i\sqrt{\pi} 2(\tilde{\Delta}_r/\sin \theta) w(z)}{\left\{ 1 + (8\tilde{\Delta}_r^2/\sin^2 \theta)[1 + i\sqrt{\pi} z w(z)] \right\}^{1/2}} \right], \quad (2)$$

$$z = 2[\Omega \tilde{\Delta} + i(\Lambda/v) \gamma] / \sin \theta; \quad \theta = \angle(\mathbf{p}, \mathbf{H}), \quad (3)$$

$$\Lambda = (2eH)^{-1/2}, \quad \tilde{\Delta} = \Delta \Lambda / v, \quad \Omega = \omega / \Delta, \quad (4)$$

$$\tilde{\Delta}^2 = (H_{c2} - H) / 6\beta_A H, \quad \Delta^2 = \Delta_0^2(T) [1 - (H/H_{c2})], \quad (5)$$

$$w(z) = \exp(-z^2) \operatorname{erfc}(-iz). \quad (6)$$

$$\tilde{\Delta}_r = \tilde{\Delta}/D, \quad D(\Omega) = 1 - \int_0^{\pi/2} d\theta 2(\Lambda\gamma/v)\sqrt{\pi} w(z). \quad (7)$$

Here $\Delta_0(T)$ is the s-wave gap in zero field, H is the spatial average of the magnetic field, $\Delta^2 = <|\Delta|^2>$, where $\Delta(r)$ is Abrikosov's vortex lattice order parameter, and β_A is the Abrikosov parameter. For the total impurity scattering rate γ we employ the Born approximation, $\gamma = \Gamma \bar{A}$ where $\Gamma = 1/2\tau_n$ and \bar{A} is the average of A over the Fermi surface which is calculated self-consistently. For a spherical Fermi surface (FS), $v \sin \theta$ is the component of the Fermi velocity $\mathbf{v}(\mathbf{p})$ perpendicular to the field \mathbf{H} . For a cylindrical FS parallel to \mathbf{c} and field $\mathbf{H} \parallel \mathbf{c}$, one has to take $\theta = \pi/2$ and v equal to the Fermi velocity in the ab-plane. For a general FS, $v \sin \theta$ is replaced by the component $v_{\perp}(\mathbf{p})$ perpendicular to the field. The gap renormalization function D in Eq.(7) was first calculated by U. Brandt¹⁰ from the ladder summation of impurity interaction lines bridging the vertices at Δ and Δ^* occurring in the self energy part $G_{\omega}^0 \Delta G_{-\omega}^0 \Delta^* G_{\omega}^0$ in Gorkov's integral equation for G . In the P-approximation scheme D takes the form given in Eq.(7) which, near H_{c2} , tends to the function introduced in Ref. 17.

The field dependence of the DOS, A , and the "coherence factor" function, B , are governed by the quantity $\tilde{\Delta} = \Delta \Lambda / v = (2\pi)^{-1/2} a / \xi$ where $a = (2/\pi)^{1/2} \Lambda$ is the lattice constant of the Abrikosov vortex lattice and $\xi = v / \Delta \pi$ is the effective coherence length in the plane perpendicular to \mathbf{H} . For $H \rightarrow H_{c2}$ and $H \rightarrow 0$ one obtains the limiting values $\tilde{\Delta} \rightarrow 0$ and $\tilde{\Delta} \rightarrow \infty$, respectively. The relationships between $\tilde{\Delta}$ and H/H_{c2} and between Δ and H/H_{c2} given in Eq.(5) have been derived from the GL-theory which is valid near H_{c2} . To get the general relationship at lower fields we make use of the gap equation in the P-approximation.¹⁸ At $T = 0$ this equation can be rewritten in the following form:

$$\int_0^{\infty} d\Omega [B(\Omega) - C(\Omega)] = 0. \quad (8)$$

Here $B(\Omega)$ is the spectral function of F given in Eq. (2) and $C(\Omega)$ is obtained by taking the limit of B for $H \rightarrow H_{c2}$ where $\Delta \rightarrow 0$:

$$C(\Omega) = \operatorname{Re} \left[-i\sqrt{\pi} 2(H/H_{c2})^{1/2} (\tilde{\Delta}_r / \sin \theta) w \left[(H/H_{c2})^{1/2} z \right] \right] \Big|_{\Lambda(H_{c2})}. \quad (9)$$

The gap equation Eq. (8) in the P-approximation corresponds to the gap equation in the BPT-approximation¹⁰ with the function B replaced by the spectral function of F derived for the theory of NMR.¹¹ Thus Eq. (8) is an implicit equation for H/H_{c2} as a function of $\tilde{\Delta}$ for given impurity scattering rate $\delta = \Gamma/\Delta_0$. This calculation is rather complicated because the impurity scattering self energy $\gamma = \Gamma \bar{A}(\Omega)$ occurring in the expression for $B(\Omega)$ in Eq. (2) has to be calculated self-consistently for each value of Ω from the expression for $A(\Omega)$ (see Eq. (1)). For $\mathbf{H} \parallel \mathbf{c}$ and a cylindrical FS one has to set $\theta = \pi/2$ in Eq.(8), and for a spherical FS Eq.(8) is averaged over the polar angle θ . In Fig. 1 we show our results for H/H_{c2} versus $\tilde{\Delta}$ obtained from Eq.(8) for $\theta = \pi/2$ and for $\delta = 0.1, 0.5$, and 1.0 . These results can be fitted very well by the relationship $H/H_{c2} = (1 + 6\beta_A \tilde{\Delta}^2)^{-1}$ [see Eq.(5)] over the whole field range if one takes $\beta_A = 1.1, 1.4$, and 1.7 for $\delta = 0.1, 0.5$, and 1.0 . Similar results are obtained for a spherical FS if one averages Eq.(8) over the polar angle θ .

In Fig. 2 we have plotted our numerical results for the normalized DOS at zero energy, $A(\Omega = 0) = \gamma_s(H)/\gamma_n$, versus H/H_{c2} where γ is the specific heat coefficient. Here we have approximated $\tilde{\Delta}$ occurring in Eq. (1) by the analytical expression in Eq. (5) with $\beta_A = 1.1, 1.4$, and 1.7 for bare impurity scattering rates $\delta = \Gamma/\Delta_0 = 0.1, 0.5$, and 1.0 (curves from top to bottom). Here we have employed the Born approximation for the total impurity scattering self energy, $\gamma = \Gamma \bar{A}(0)$, where $\bar{A}(0)$ is calculated self-consistently. This means that δ is replaced by $\delta \bar{A}(0)$. For $\delta = 0.1$ and $\theta = \pi/2$ the function $A(0)$ is close to the clean limit result shown in Ref. 18 for the s-wave pairing state. The latter function has been shown to be very close to the numerical solution of the Eilenberger equations over the whole field range from H_{c2} to $H = 0$ corresponding to H_{c1} . One can see that all curves in Fig. 2 tend to zero in

the limit $H/H_{c2} \rightarrow 0$, which is due to the gap renormalization. For a spherical FS one has to average Eq.(1) over the polar angle θ . For the plot of A versus H/H_{c2} one needs Eq.(5) where β_A is calculated from the θ -angle average of Eq.(8). We find that the results are very similar to the $\theta = \pi/2$ results in Fig. 2.

We turn now to the theory of the electronic thermal conductivity κ_e in the vortex state which has been developed in Ref. 7 by replacing the zero-field Green's functions G and F in the theory of Ref. 15 by the Green's functions of the BPT-approximation. This theory has been applied to superconducting states with nodes in the gap such as Sr_2RuO_4 , the cuprates, and UPt_3 . To save space we omit here the expression for κ_e . The main features of this expression are the following. Most important is the term $\text{Im } \varepsilon_0$ in the denominator of the ω -integral with the well-known factor $\omega^2 \text{sech}^2(\omega/2T)$. This term $\text{Im } \varepsilon_0$ corresponds to the scattering rate of quasiparticles due to impurity and Andreev scattering. The other term corresponds to the coherence factor of BCS theory. In the zero field limit both terms in the expression of Ref. 7 tend correctly to those occurring in the expression of Ref. 15. The physical meaning of $\text{Im } \varepsilon_0$ is the following. The equation for the position, ε_0 , of the pole of the Green's function G in the BPT-approximation⁹ yields $\text{Im } \varepsilon_0 = \gamma + \gamma_A$ where γ is the total impurity scattering rate and γ_A is the imaginary part of the quasiparticle self energy Σ_ω at ε_0 . From the kernel of Gorkov's integral equation for G one sees that, in the spatial representation, $\Sigma_\omega(r_1, r_2) = -V(r_1, r_2)G_{-\omega}^0(r_1 - r_2)$, where $V(r_1, r_2) = \Delta(r_1)\Delta^*(r_2)\exp(-i\int_1^2 2eA \cdot ds)$ and $\Delta(r)$ is Abrikosov's vortex lattice order parameter. From this expression one recognizes that $\gamma_A = -\text{Im } \Sigma_\omega$ is the scattering rate for converting a quasiparticle into a quasi-hole by Andreev reflection at $\Delta^*(r_2)$ and then back into a quasiparticle at $\Delta(r_1)$. The Fourier transform of Σ_ω with respect to the difference coordinate $(r_1 - r_2)$ is equal to

$$\Sigma_\omega(p) = -\int d^3p' V(p')G_{-\omega}^0(p - p'), \quad (10)$$

with

$$V(p') = 8\pi^2\Delta^2\Lambda^2\delta(p'_z)\exp[-\Lambda^2(p'^2_x + p'^2_y)] \quad (\hat{\mathbf{z}} \parallel \mathbf{H}). \quad (11)$$

For a spherical Fermi surface the result is⁹

$$\Sigma_\omega(p) = -i\sqrt{\pi}\Delta^2(\Lambda/v \sin \theta)w[(\omega + i\gamma + \varepsilon)\Lambda/v \sin \theta] \quad (12)$$

where ε is the normal state energy measured from the Fermi energy, $\theta = \angle(\mathbf{p}, \mathbf{H})$, and γ is the total impurity scattering self energy.

In the $\omega \rightarrow 0$ limit corresponding to $T \rightarrow 0$ one obtains the following explicit expression for $\text{Im } \varepsilon_0$:^{7,10}

$$\begin{aligned} \text{Im } \varepsilon_0 &= \gamma + \gamma_A; \quad \gamma_A = (v/\Lambda)\beta \\ \beta &= \tilde{\Delta}_r^2 \left\{ \left[(\gamma\Lambda/v)^2 + \tilde{\Delta}_r^2 + \eta \sin^2 \theta \right]^{1/2} + (\gamma\Lambda/v) \right\}^{-1}; \quad (\pi^{-1} \leq \eta \leq 1/2). \end{aligned} \quad (13)$$

All the other quantities $\tilde{\Delta}$ and β occurring in the expression for κ_e (see Eq.(13) of Ref. 7)) are also renormalized by the replacement $\tilde{\Delta} \rightarrow \tilde{\Delta}_r$ (see Eq.(7) for $\Omega = 0$). Note that $\tilde{\Delta} \sim a/\xi$ and $\Gamma\Lambda/v \sim a/\ell$. In Fig. 3 we have plotted our results for κ_{es}/κ_{en} versus H/H_{c2} in the limit $T \rightarrow 0$. The bare impurity scattering rates $\delta = \Gamma/\Delta_0$ are 0.1, 0.5, and 1.0 (from bottom to top). For a spherical FS one has to evaluate the average of κ_e over the polar angle θ which yields nearly the same results as shown in Fig. 3 for the plots of κ_{es}/κ_{en} vs H/H_{c2} if one uses Eq.(5) with the β_A calculated from the average of Eq.(8). All curves tend to zero in the limit $H/H_{c2} \rightarrow 0$. One sees that, for low impurity scattering rates, κ_{es}/κ_{en} exhibits a strong upward curvature near H_{c2} which is caused by the rapid reduction of the Andreev scattering rate γ_A with decreasing $\tilde{\Delta}$ or increasing field as can be seen from Eq. (13). For increasing impurity scattering rate γ this effect is diminished because γ_A becomes smaller in comparison to γ as can be seen from the expression in Eq. (13).

The main problem in analyzing the measured thermal conductivity κ in the mixed state is to separate the electronic and phononic contributions κ_e and κ_{ph} .⁴ The general expression for κ_{ph} (see Eq. (4) of Ref. 8) contains, in addition to other phonon relaxation times due to defect scattering, the relaxation time $\tau_p(\omega)$ due to scattering of phonons of frequency ω by quasiparticles which changes drastically in the BCS state. The expression for $1/\tau_{ps}$ in the BCS state¹⁶ has been extended to the vortex lattice state by replacing the BCS DOS E/ε , where $\varepsilon = (E^2 - \Delta^2)^{1/2}$, and the function Δ/ε occurring in the BCS coherence factor, with the spectral functions A and B of Eqs. (1) and (2). In the zero field limit the latter expressions tend correctly to the BCS functions with $\omega \equiv E$. The resulting ratio of phonon relaxation times in the normal and mixed states is given by (see Eq. (3) of Ref. 8):

$$\begin{aligned} \tau_{pn}/\tau_{ps} &= g(\Omega_0) = [1 - \exp(-\Omega_0/y)](2/\Omega_0) \int_0^\infty d\Omega f[(\Omega - \Omega_0/2)/y] f[-(\Omega + \Omega_0/2)/y] \\ &\quad \times [A(\Omega - \Omega_0/2)A(\Omega + \Omega_0/2) - B(\Omega - \Omega_0/2)B(\Omega + \Omega_0/2)]. \end{aligned} \quad (14)$$

Here, $\Omega_0 = \omega_0/\Delta$ is the phonon energy ω_0 divided by $\Delta = \Delta(T, H)$, f is the Fermi function, and $y = T/\Delta(T, H)$. In Ref. 8 we calculated g in the limit $T \rightarrow 0$. It was found that in the limit $\tilde{\Delta} \rightarrow \infty$, or $H/H_{c2} \rightarrow 0$, g tends correctly to the BCS step function with a step at $\Omega_0 = 2$, or $\omega_0 = 2\Delta$. This step function is washed out as $\tilde{\Delta} \rightarrow 0$, or $H/H_{c2} \rightarrow 1$, and it tends to the constant, 1. Since it is important to know the temperature dependence of κ_{ph} , and thus of $\tau_{pn}/\tau_{ps} = g$, for analyzing the measured κ as a function of T at fixed field,⁴ we have now calculated the T -dependence of the expression in Eq.(14). For this purpose we make use of the fact that, according to the general expression for κ_{ph} (see Eq.(4) of Ref. 8), the maximum of the integrand in that x -integral occurs at about $x_m = \omega_{0m}/T \simeq 4$. Therefore it is a good approximation to make the variable transformations $\Omega_0 = x_m y$ and $\Omega = ty$ with $y = T/\Delta(T, H)$ in Eq.(14). This yields $\tau_{pn}/\tau_{ps} = g(x_m y)$ as a function of the T -dependent quantity y for fixed $\tilde{\Delta}$, or field H/H_{c2} . In Fig. 4 we have plotted $g(x_m y)$ versus $y = T/\Delta(T, H)$ for constant $x_m = 4$ and constant $\tilde{\Delta} = 0.2$, 0.3, and 0.6, or $H/H_{c2} = 0.78$, 0.62, and 0.29 (see Fig. 1) for $\delta = 0.1$. In the limit $\tilde{\Delta} \rightarrow \infty$, or $H/H_{c2} \rightarrow 0$, one obtains a step function with a step at $y = 1/2$, that is, $\Omega_0 = 4y = 2$ or $\omega_0 = 2\Delta$, as it should be. One sees, that for intermediate values of the field, $\tau_{pn}/\tau_{ps} = g$ considered as a function of T is smeared out and tends to one for high fields. In the limit $y \rightarrow 0$, or $\Omega_0 \rightarrow 0$ Eq.(14) yields $g(\Omega_0 = 0) = [A(\Omega_0 = 0, \tilde{\Delta}, \theta)]^2$. If the scattering rate $1/\tau_{ps} = (1/\tau_{pn})g$ occurring in the denominator of the ω -integral in the expression for κ_{ph} (see Eq.(4) in Ref. 8) is comparable to or larger than the other scattering rates due to phonon-defect scattering, we expect that κ_{ph} rapidly decreases for increasing field for temperatures smaller or close to $T \simeq (1/2)\Delta(T, H)$. In the measurements of κ one observes a fast drop of κ in small fields at temperatures around $T_c/6$ ⁴ which can be attributed to the fast drop of κ_{ph} due to scattering by quasiparticles in the π -band vortex lattice.

It is interesting to compare the temperature dependence of the phonon lifetime τ_p with the lifetime τ_e of a quasiparticle due to scattering by acoustic phonons. This scattering rate has been derived for the BCS state in Ref. 19 (see Eq.(3.9)). We extend this expression for the scattering rate $1/\tau_{es}$ in analogy to our procedure for $1/\tau_p$ from the BCS to the vortex state by replacing the density of states by the DOS $A(\Omega)$ in Eq.(1) and the coherence factor terms by $B(\Omega)$ in Eq.(2). Then we obtain:

$$1/\tau_{es}(\omega) = C[f(-\beta\omega)]^{-1}A^{-1}(\Omega) \int_0^\infty d\omega_0 \omega_0^2 \{A(\Omega)A(\Omega - \Omega_0) - B(\Omega)B(\Omega - \Omega_0) \\ \times f[-\beta(\omega - \omega_0)][1 + b(\beta\omega_0)] \\ + [A(\Omega)A(\Omega + \Omega_0) - B(\Omega)B(\Omega + \Omega_0)]f[-\beta(\omega + \omega_0)]b(\beta\omega_0)\}. \quad (15)$$

Here C is a constant arising from the electron-phonon matrix elements, $\beta = 1/T$, $b(x) = (e^x - 1)^{-1}$, and ω_0 is the phonon frequency. We use this expression now in the calculation of the electronic thermal conductivity κ_e . We mentioned above that the integrand of the ω -integral in the expression for κ_e given in Ref. 7 contains the term $\text{Im}\varepsilon_0 = \gamma + \gamma_A$ in the denominator which corresponds to the sum of relaxation rates of a quasiparticle due to impurity and Andreev scattering. The effect of thermal scattering by phonons can now be taken into account by adding $1/\tau_{es}$ to $\text{Im}\varepsilon_0$. The temperature dependence of κ_e is governed by the factor $(\omega/T)^2 \text{sech}^2(\omega/2T)$ in the integrand of the ω -integral which yields the main contribution of the integrand from the vicinity of $x = \omega/T$ at about $x_m = 2$. Therefore we can estimate the temperature dependence of $1/\tau_{es}$ by carrying out the following variable transformations in Eq.(15): $x = \omega/T$, $t = \omega_0/T$, $\Omega = xy$, and $\Omega_0 = ty$ with $y = T/\Delta(T, H)$. This yields $1/\tau_{es}$ as a function of $\Omega = xy$ and x . The normal state relaxation rate $1/\tau_{en}$ is obtained from Eq.(15) by setting $A = 1$ and $B = 0$. In Fig. 5 we have plotted τ_{es}/τ_{en} as a function of $y = T/\Delta(T, H)$ for constant $x = x_m = 2$ and $\tilde{\Delta} = 0.2$, 0.3, and 0.6 ($H/H_{c2} = 0.78$, 0.62, and 0.29, for $\delta = 0.1$, see Fig. 1). One sees that for increasing $\tilde{\Delta}$, or decreasing field, this function tends to a step function where the step occurs at $y = 1/2$, that is, at a quasiparticle energy $\Omega = \omega/\Delta = 1$. This result agrees with the previous result for the BCS state.¹⁹ One recognizes that the variations of τ_{en}/τ_{es} as a function of y are much smaller than those of the phonon lifetime ratio τ_{pn}/τ_{ps} shown in Fig. 4 where, for increasing $\tilde{\Delta}$, a step occurs at about $y = \Omega/4 = 1/2$, i.e., at a phonon energy $\Omega_0 = \omega_0/\Delta = 2$. The contribution of $1/\tau_{es}$ to the relaxation rate $\text{Im}\varepsilon_0$ occurring in the electronic thermal conductivity κ_e increases with temperature like T^3 because $1/\tau_{en}$ is proportional to T^3 . In the presence of moderate impurity scattering this becomes comparable with γ only at temperatures such that $y = T/\Delta(T, H) > 1$ where, according to Fig. 5, the ratio τ_{en}/τ_{es} is nearly one. The expression for $1/\tau_{es}$ in Eq.(15) has been calculated in analogy to Ref. 19 for quasiparticle scattering by acoustic phonons. Instead of this spectrum, $C\omega_0^2$, one should employ in the expression for $1/\tau_{es}$ the transport Eliashberg functions $\alpha_{tr}^2 F_{nn}(\omega_0)$, where $n = \sigma, \pi$, which have been calculated for MgB₂.²¹ Since the coupling constant $\lambda_{\sigma\sigma} = 0.81 > \lambda_{\pi\pi} = 0.41$, we conclude that for the σ -band the field dependence of $1/\tau_{es}$ should be taken into account while, for the π -band, $1/\tau_{es}$ can safely be approximated by $1/\tau_{en}$.

III. CONCLUSIONS

We have calculated the density of states $A(\omega)$, the electronic thermal conductivity κ_e , and the scattering rates $1/\tau_p(\omega)$ of a phonon and $1/\tau_e(\omega)$ of a quasiparticle for a single isotropic gap over the entire field range of the mixed state. That the BPT^{9–11} and P¹² methods for these calculations are valid approximation schemes has been proved by comparison of the results for A with the solutions of the Eilenberger equations for Abrikosov's vortex lattice order parameter.¹⁸ By solving the gap equation including impurity self energy and vertex corrections (see Fig. 1), we have shown that the relation between the central parameter of the theory, $\tilde{\Delta} = \Delta \Lambda/v$, and H/H_{c2} can be very well approximated by the Ginzburg-Landau (GL) relation [see Eq.(5)] over the entire field range if one uses an appropriate value of the Abrikosov parameter β_A . This result is connected with the fact that the Abrikosov order parameter is a solution of the linearized GL equations which allows extension of the BPT method over the entire region of linear magnetization.²²

The second main result of the present paper is that the vertex corrections due to impurity scattering^{10,12} substantially reduce the dependence of the functions $\gamma_s(H)/\gamma_n$, $\kappa_{es}(H)/\kappa_{en}$, and $\tau_{pn}/\tau_{ps}(H)$ on the amount of impurity scattering. The impurity scattering rate $\delta = \Gamma/\Delta_0 = (\pi/2)(\xi_0/\ell)$ (ξ_0 is the coherence length and ℓ the mean free path) is renormalized here in the Born approximation $\Gamma \rightarrow \gamma = \Gamma A(\omega)$ where $A(\omega)$ is calculated self-consistently from Eq.(1). The vertex corrections yield a renormalization of the gap $\tilde{\Delta}_r$ due to the function D [see Eq.(7)]. As can be seen from Fig. 2, the functions $\gamma_s(H)/\gamma_n$ for $\delta = 0.1$, 0.5, and 1.0 are not very different from each other. The results are however quite different if we set the renormalization function D equal to one. Then the slope of $\gamma_s(H)/\gamma_n$ versus H/H_{c2} at $H = 0$ rises rapidly with δ and becomes very large for $\delta = 1$. It should be noticed that all curves in Fig. 2 tend to zero in the zero field limit as they should to be in accordance with Anderson's theorem for "dirty" superconductors. Our result that the effect of impurity scattering on the field dependence of $\gamma_s(H)/\gamma_n$ for a single isotropic gap is rather small and does not yield a rapid rise for small fields, gives support for the two-gap model in interpreting the measurements of $\gamma_s(H)/\gamma_n$ on single crystals of MgB₂.³ According to this model, the first steep increase of $\gamma_s(H)/\gamma_n$, which is nearly the same for applied fields parallel and perpendicular to the c-axis, arises from the behavoir of the small gap associated with the three dimensional π -band. This in effect closes for increasing field due to the overlap of the vortex cores with large radius $\xi_\pi \sim 500\text{\AA}$ ⁶ at a relatively small "virtual" upper critical field $H_{c2}^S \sim 3 - 4$ kOe. The remaining superconducting contribution above H_{c2}^S arises from the large gap associated with the two dimensional σ -band which closes at an upper critical field $H_{c2}^{(c)} \sim 32$ kOe and $H_{c2}^{(ab)} \sim 160$ kOe. The field dependence of the π -band and the σ -band contributions to $\gamma_s(H)/\gamma_n$ is presumably given by the almost linear curves in Fig. 2 for $\delta = 1.0$ and $\delta = 0.5$ with H_{c2} equal to H_{c2}^S and $H_{c2}^{(c)}$ or $H_{c2}^{(ab)}$, respectively.

The results for $\kappa_{es}(H)/\kappa_{en}$ shown in Fig. 3 depend on the impurity scattering rate δ primarily because the effect of Andreev scattering on the upward curvature becomes relatively smaller as δ increases. Although the slope at $H = 0$ is relatively small even for $\delta = 1$, it becomes very large at $\delta = 1$ if the renormalization of the gap $\tilde{\Delta}_r = \tilde{\Delta}/D$ due to the vertex correction D in κ_e [see Eq.(13)] is neglected. This result has the consequence that the observed steep rise of $\kappa_e(H)$ for small fields parallel or perpendicular to the c-axis in single-crystalline MgB₂⁴ can again be explained only in terms of the two-gap model where the smaller gap in the three dimensional π -band closes in effect at a "virtual" upper critical field $H_{c2}^S \sim 3 - 4$ kOe due to the overlap of the vortex cores with large radius ξ_π .⁶ At higher fields $\kappa_e(H)$ tends to saturate until, in the vicinity of $H_{c2}^{(c)} \sim 32$ kOe, the contrubution to κ_e from the larger gap associated with the cylindrical σ -band exhibits an upward curvature. The contributions to κ_e arising from the π - and σ -bands are presumably given by the curves in Fig. 3 for $\delta = 1.0$ and $\delta = 0.5$ with the corresponding H_{c2} equal to H_{c2}^S and $H_{c2}^{(c)}$ where the curve for $\delta = 0.5$ yields the measured upward curvature near H_{c2} .

The rapid decrease of κ observed at low fields, which is attributed to the decrease of the phononic thermal conductivity κ_{ph} ,⁴ can be explained by the field and relevant temperature dependence of the ratio of phonon lifetimes $\tau_{pn}/\tau_{ps}(H) = g(H)$ shown in Fig. 4. One sees that $g(H)$ tends rapidly to the constant one for increasing field and values of $y < 1/2$ corresponding to temperatures $T < (1/2)\Delta(T, H)$. If we assume that Δ is the smaller gap associated with the π -band, then the T satisfying this condition are much smaller than T_c . However, at the lowest temperatures, this effect on κ_{ph} is strongly reduced because the scattering rate $1/\tau_{ps}$ occurring in the denominator of the ω -integral for κ_{ph} is multiplied by T/T_c in comparison to the scattering rate due to sample boundary scattering (see Eq.(4) of Ref. 8).

We have calculated $\kappa_e(H)$ in the limit $T \rightarrow 0$, or $\omega \rightarrow 0$. For finite T one has to solve the transcendental equation determining the pole ε_0 of the BPT-Green's function⁷ for each finite value of ω occurring in the ω -integral for κ_e . It should be pointed out that this calculation is avoided in the expression for κ_e which was derived from linear response theory.^{13,14} For higher temperatures one should add to the sum of scattering rates γ and γ_A due to impurity and Andreev scattering [see Eq.(13)], the scattering rate $1/\tau_{es}(H)$ due to scattering of quasiparticles by phonons. The field and relevant temperatur dependence of the ratio $\tau_{en}/\tau_{es}(H)$ is shown in Fig. 5 as a function of $y = T/\Delta(T, H)$.

One sees that this ratio is nearly equal to one for values of $y > 1$ corresponding to temperatures $T > \Delta(T, H)$. For the small gap associated with the π -band this condition is probably satisfied at those temperatures where $1/\tau_{en} \sim T^3$ becomes comparable to the intraband impurity scattering γ for the π -band. However, for the large gap associated with the σ -band, this condition might not be satisfied. We conclude from these estimates that, for the π -band, $1/\tau_{es}$ can be approximated by $1/\tau_{en}$ while, for the σ -band, the field dependence of $1/\tau_{es}(H)$ should be taken into account. These considerations are supported by detailed calculations which yield a larger intraband impurity scattering rate γ for the π -band than for the σ -band,²⁰ and a larger scattering rate $1/\tau_{en}$ for the σ -band than for the π -band because the intraband electron-phonon coupling constant satisfies $\lambda_{\sigma\sigma} > \lambda_{\pi\pi}$.²¹

Our assumption that we can simply add our results obtained for two different isotropic gaps and different upper critical fields in the π - and σ -bands is a crude approximation in view of the actual situation in MgB₂. It is true that the interaction due to interband impurity scattering between the σ - and π -bands is small.²⁰ However, we have neglected the pairing interaction between the two bands which presumably leads to Cooper pair tunneling from the σ -band with strong pairing to the π -band where it leads to giant vortex cores and where superconductivity is maintained above the virtual H_{c2}^S up to H_{c2} .⁵ Nevertheless we believe that our clear-cut results for the mixed state of a single isotropic gap are helpful in analyzing the complicated behavior of different physical quantities in MgB₂.

Another approximation is that we have neglected higher harmonic oscillator components N of Abrikosov's vortex lattice order parameter which lead to a distortion of the lattice at lower fields.¹⁸ For an s-wave superconductor the BPT method breaks down at low fields where properties are determined by the states bound to the vortex cores. However, STS measurements in MgB₂ show an absence of localized states in the cores.⁶

We would like to thank T. Dahm and K. Scharnberg for valuable discussions.

¹ J. Nagamatsu, N. Nakagawa, T. Muranaka, Y. Zenitani, and J. Akimitsu, *Nature* **410**, 63 (2001).
² H. D. Yang, J.-Y. Lin, H. H. Li, F. H. Hsu, C. J. Liu, S.-C. Li, R.-C. Yu, and C.-Q. Jin, *Phys. Rev. Lett.* **87**, 167003 (2001).
³ F. Bouquet, R. A. Fisher, N. E. Phillips, D. G. Hinks, and J. D. Jorgensen, *Phys. Rev. Lett.* **87**, 047001 (2001); cond-mat/0207141 (unpublished).
⁴ A. V. Sologubenko, J. Jun, S. M. Kazakov, J. Karpinski, and H. R. Ott, *Phys. Rev. B* **66**, 014504 (2002).
⁵ N. Nakai, M. Ichioka, and K. Machida, *J. Phys. Soc. Jpn.* **71**, 23 (2002).
⁶ M. R. Eskildsen, M. Kugler, S. Tanaka, J. Jun, S. M. Kazakov, J. Karpinski, and Ø. Fischer, *Phys. Rev. Lett.* **89**, 187003-1 (2002).
⁷ L. Tewordt and D. Fay, *Phys. Rev. B* **64**, 24528 (2001).
⁸ L. Tewordt and D. Fay, *Phys. Rev. Lett.* **89**, 137003-1 (2002).
⁹ U. Brandt, W. Pesch, and L. Tewordt, *Z. Phys.* **201**, 209 (1967).
¹⁰ U. Brandt, PhD-thesis, Hamburg (1969); *Phys. Lett.* **27A**, 645 (1968).
¹¹ W. Pesch, PhD-thesis, Hamburg (1968); *Phys. Lett.* **28A**, 71 (1968).
¹² W. Pesch, *Z. Phys. B* **21**, 263 (1975).
¹³ P. Klimesch and W. Pesch, *J. Low Temp. Phys.* **32**, 869 (1978).
¹⁴ I. Vekhter and A. Houghton, *Phys. Rev. Lett.* **83**, 4626 (1999).
¹⁵ V. Ambegaokar and L. Tewordt, *Phys. Rev.* **134**, A805 (1964).
¹⁶ J. Bardeen, G. Rickayzen, and L. Tewordt, *Phys. Rev.* **113**, 982 (1959).
¹⁷ E. Helfand and N. R. Werthamer, *Phys. Rev.* **147**, 288 (1967).
¹⁸ T. Dahm, S. Graser, C. Iniotakis, and N. Schopohl, *Phys. Rev. B* **66**, 144515 (2002).
¹⁹ L. Tewordt, *Phys. Rev.* **128**, 12 (1962).
²⁰ I. I. Mazin et al, *Phys. Rev. Lett.* **89**, 107002-1 (2002).
²¹ Y. Kong, O. V. Dolgov, O. Jepsen, and O. K. Andersen, *Phys. Rev. B* **64**, 020501(R) (2001).
²² E. H. Brandt, *Rep. Prog. Phys.* **58**, 1465 (1995).

Fig. 1

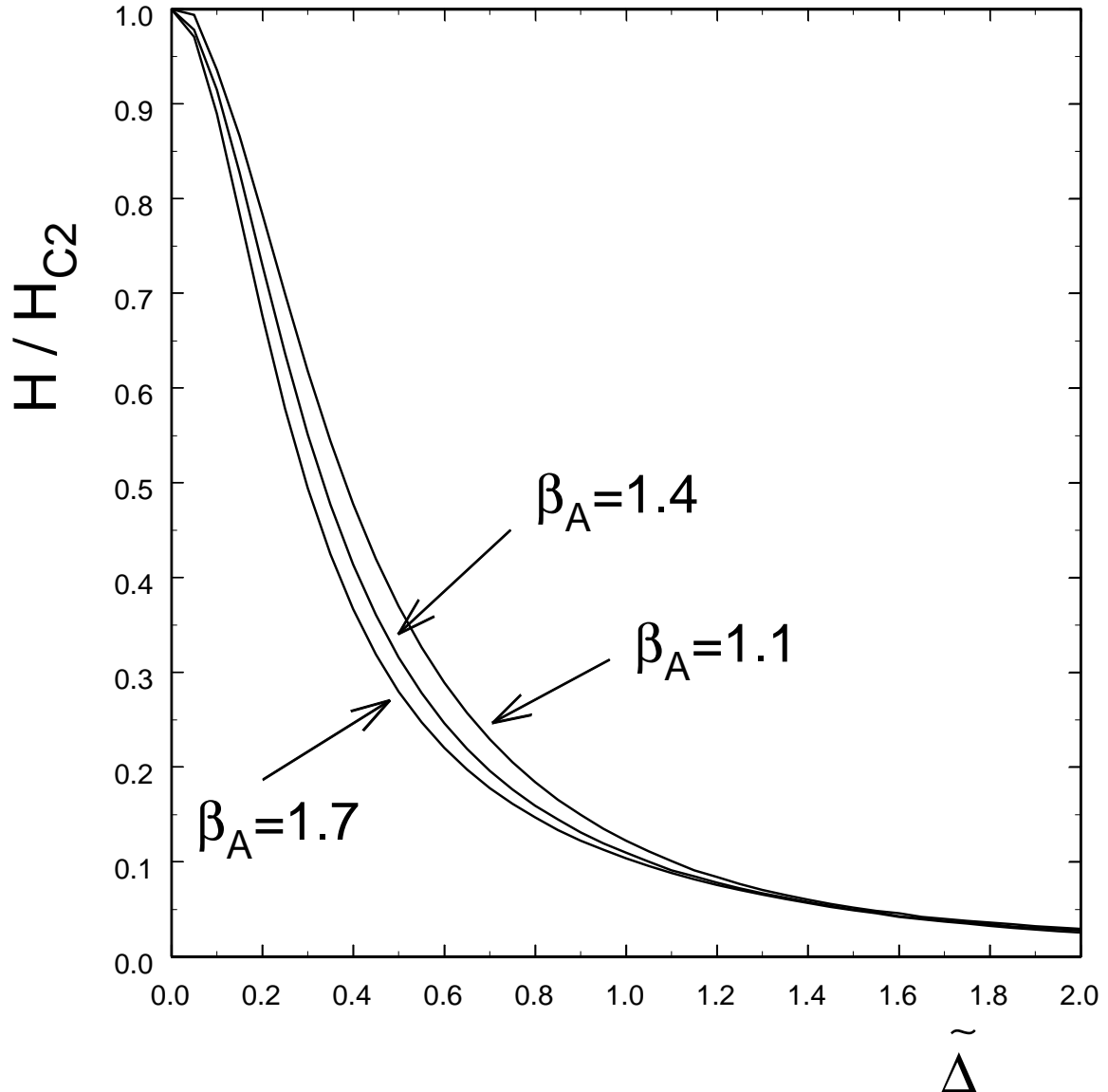


FIG. 1. Solutions of gap equation for H/H_{c2} vs $\tilde{\Delta} = \Delta\Lambda/v$ ($\Lambda = (2eH)^{-1/2}$), for impurity scattering rate $\delta = 0.1, 0.5$, and 1.0 (curves top to bottom), for $\theta = \pi/2$. The fits are obtained from the analytical expression with the Abrikosov parameter $\beta_A = 1.1, 1.4$, and 1.7 [see Eq.(5)].

Fig. 2

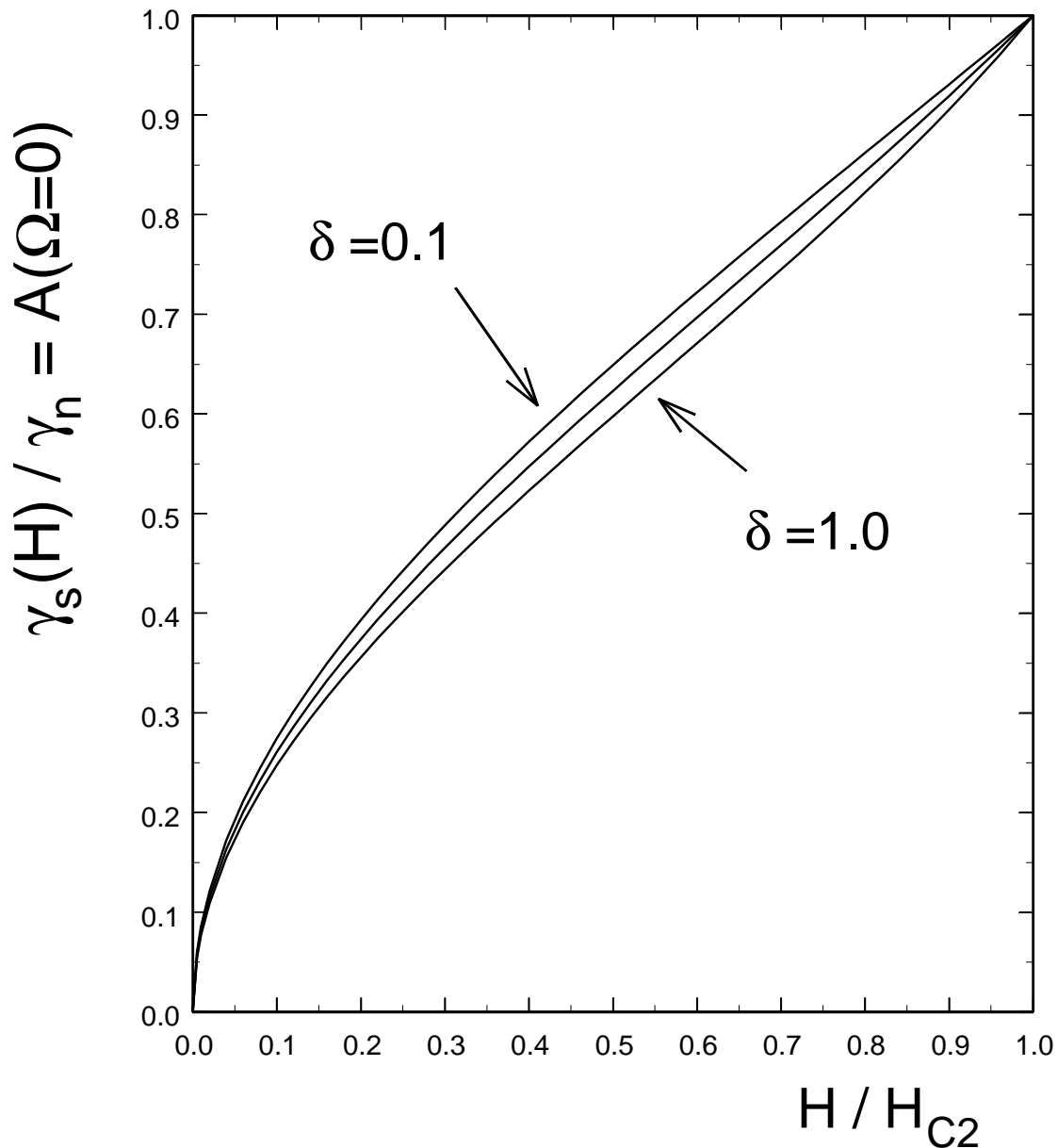


FIG. 2. Ratio of specific heat coefficients, γ_s/γ_n , vs H/H_{c2} for reduced impurity scattering rates $\delta = \Gamma/\Delta_0 = 0.1, 0.5$, and 1.0 (from top to bottom) for $\theta = \pi/2$ (cylindrical Fermi surface(FS)).

Fig. 3

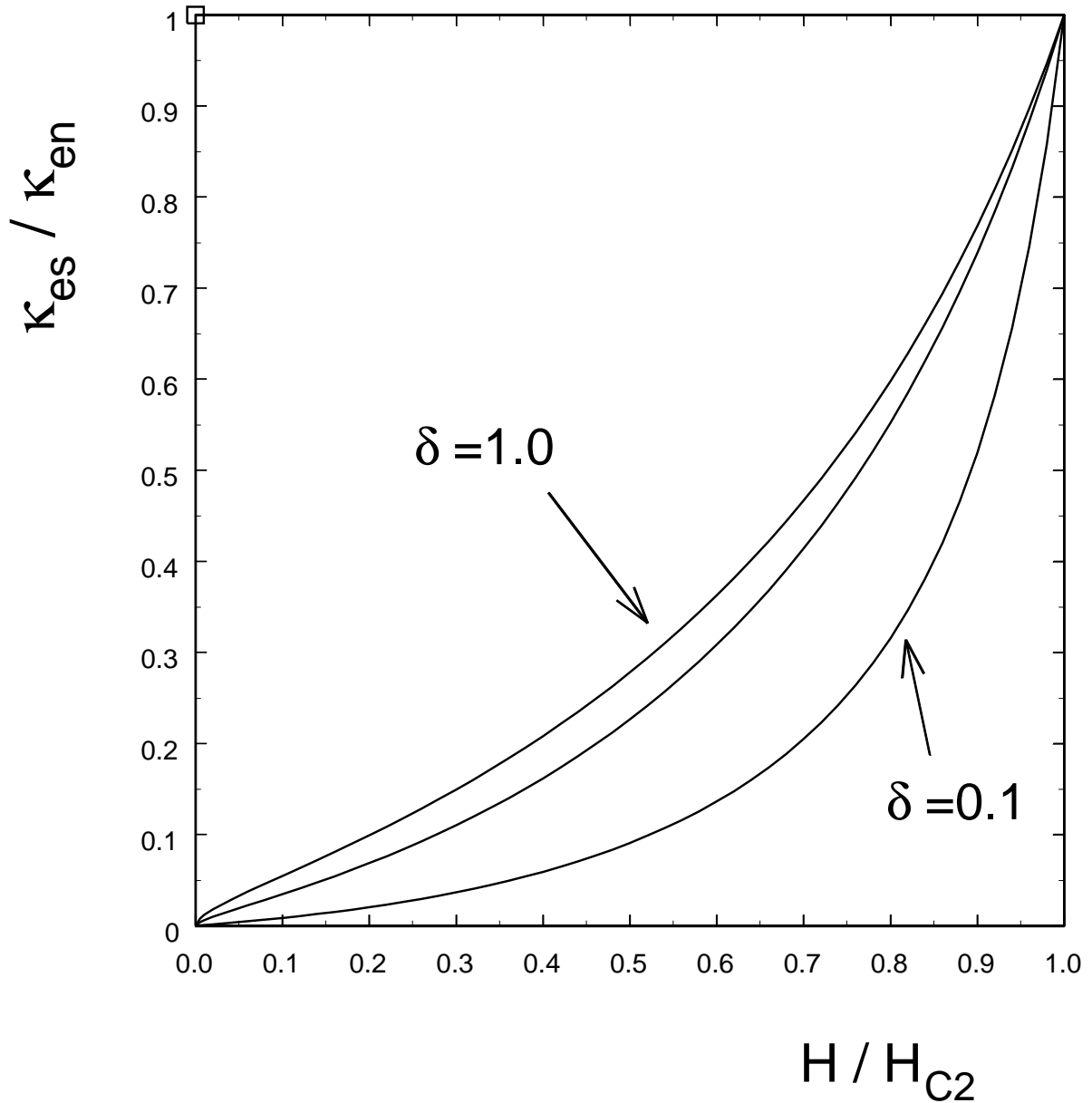


FIG. 3. Electronic thermal conductivity ratio κ_{es}/κ_{en} vs H/H_{c2} for $\delta = 0.1$, 0.5 , and 1.0 (from bottom to top. Notation as in Fig. 2).

Fig. 4

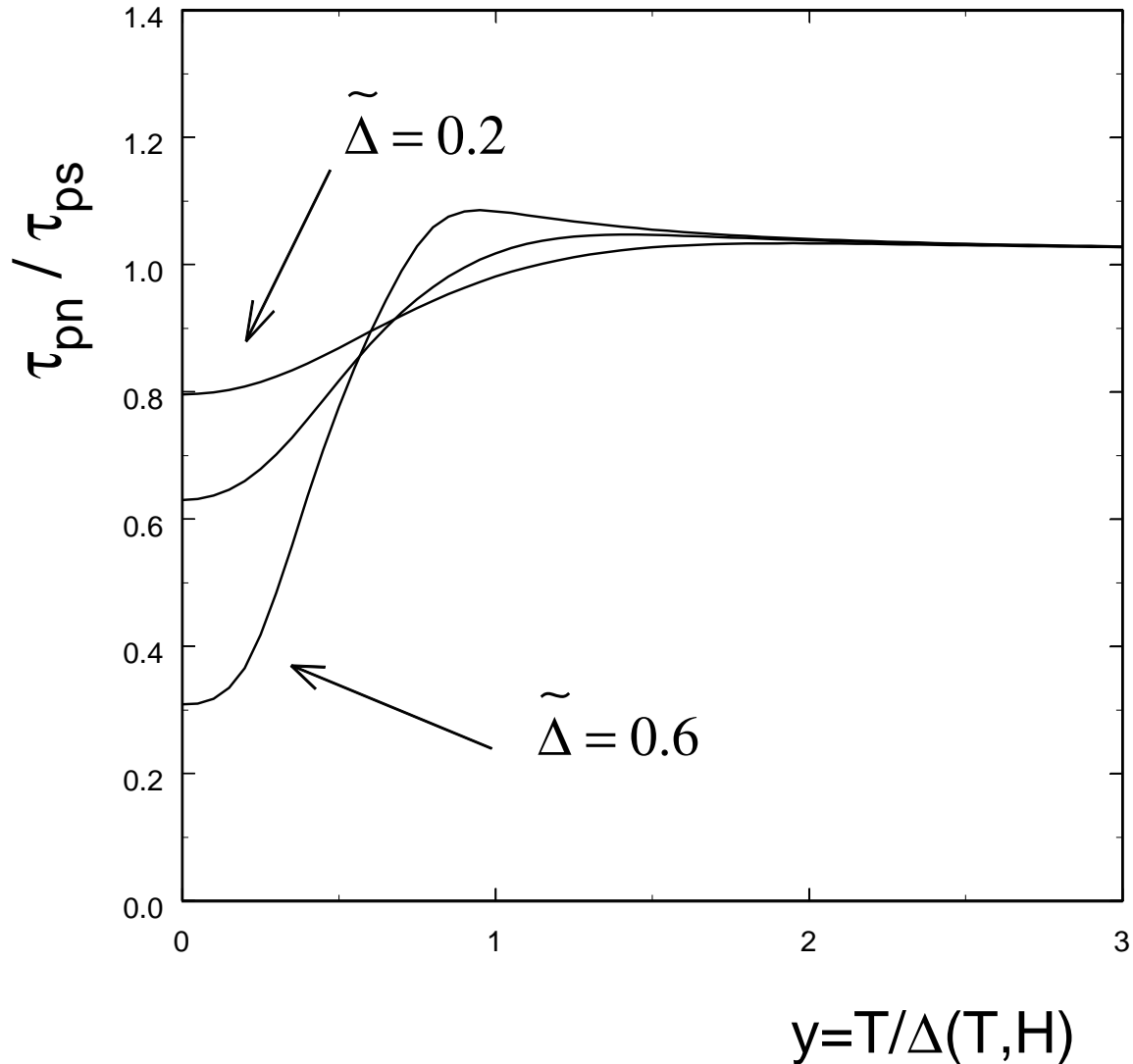


FIG. 4. Ratio τ_{pn}/τ_{ps} of phonon lifetimes vs $y = T/\Delta(T, H)$ corresponding to dominant phonon energy $\omega_0 = 4\Delta$ or $4T$ which determines the phononic thermal conductivity κ_{ph} . The constant fields are $H/H_{c2} = 0.29, 0.62, 0.78$, or, $\tilde{\Delta} = 0.6, 0.3, 0.2$ (from bottom to top) and $\delta = 0.1$.

Fig. 5

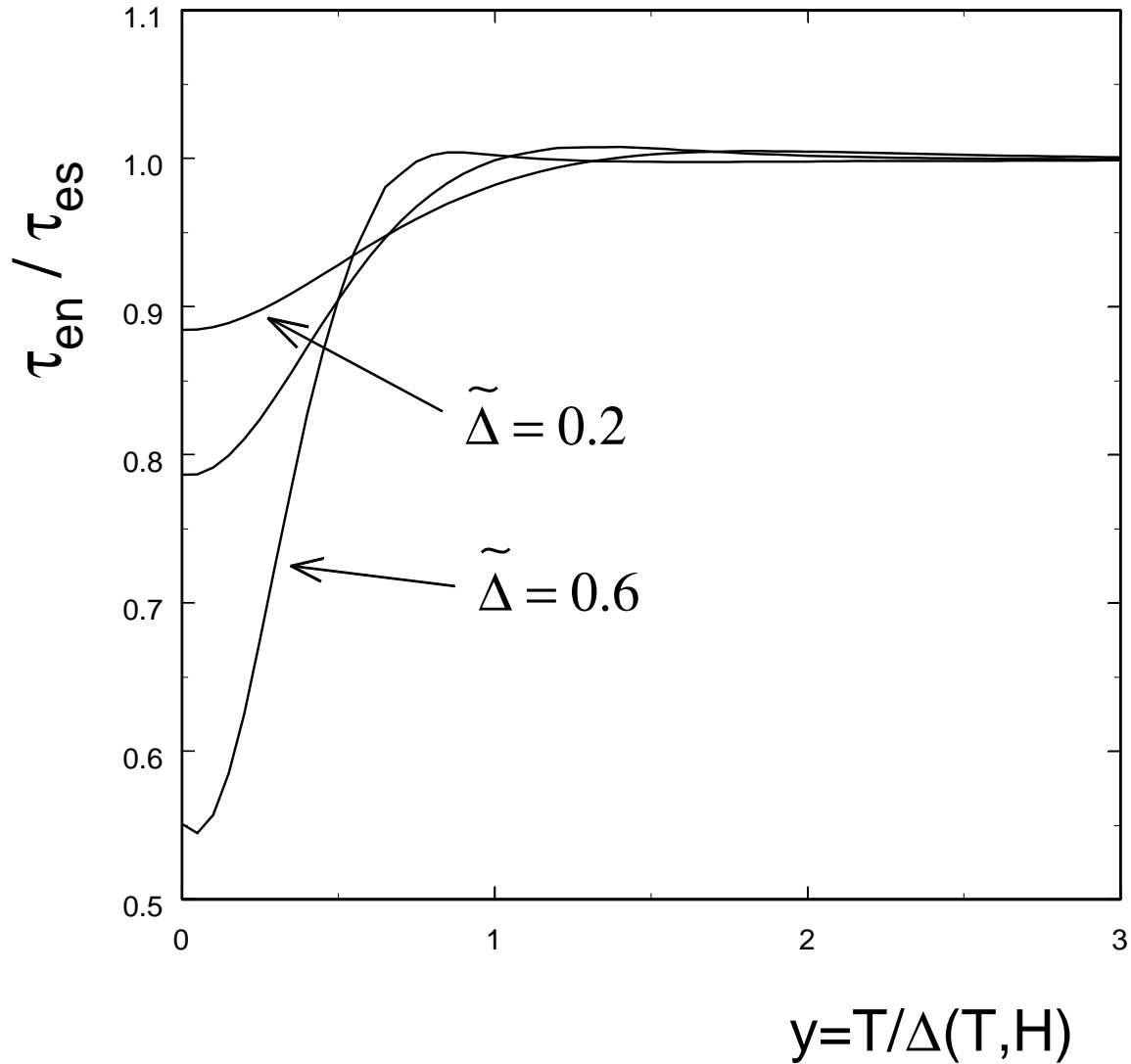


FIG. 5. Ratio τ_{en}/τ_{es} of quasiparticle lifetimes due to phonon scattering vs $y = T/\Delta(T, H)$ corresponding to dominant quasiparticle energy $\omega = 2\Delta y = 2T$ which determines the electronic thermal conductivity κ_e . The constant fields are $H/H_{c2} = 0.29, 0.62, 0.78$, or, $\tilde{\Delta} = 0.6, 0.3, 0.2$ (from bottom to top), for $\delta = 0.1$.